ACTA ONCOLOGICA, 2018
VOL. 57, NO. 5, 629–636
https://doi.org/10.1080/0284186X.2017.1400686

Taylor & Francis
Taylor & Francis Group

ORIGINAL ARTICLE

Clinical efficacy and safety of a highly conformal, supine, hybrid forward and inverse planned intensity modulated radiation therapy technique for craniospinal irradiation

Safia K. Ahmed, Jon J. Kruse, Thomas B. Bradley, Chris J. Beltran and Nadia N. Issa Laack

Department of Radiation Oncology, Mayo Clinic, Rochester, MN, USA

ABSTRACT

Purpose: To demonstrate the clinical efficacy and safety of a highly conformal, supine, hybrid forward and inverse planned intensity modulated radiation therapy (IMRT) technique for photon craniospinal irradiation (CSI).

Methods: Patients who received supine, hybrid IMRT CSI from 2009 to 2014 were included in this retrospective review. Clinical target volume (CTV) was defined as intracranial contents and thecal sac, including nerve roots. Dose was prescribed such that >99% of CTV received >99% of prescription and >95% of the planning target volume received >95% of prescription, with no attempt to include vertebral bodies. Lateral fields were utilized at the cranium and upper cervical spine. Spine fields were either single posterior or 2–3 obliques. Plans were generated with a hybrid of forward and inverse planned IMRT. Inferior borders of the cranium fields and superior border of the lower spine field were designed with 6–15 cm long, gradual dose gradients by sequential closing of multileaf collimator leaves using forward planned multiple static segment IMRT delivery. The sliding window upper spine IMRT field was created by the inverse planning system to match gradients of the brain and lower spine fields. The lower spine field gradient was similarly completed.

Results: The cohort consisted of 34 patients. Median CSI dose was 36 Gy (range: 18–39.6 Gy). With a median follow up of 59.4 months, there were no isolated recurrences or spinal myelopathies at CTV margins or field gradients. Eleven patients had recurrence, all of which were intracranial.

Conclusions: Our hybrid forward and inverse planned IMRT supine CSI technique did not result in any isolated recurrences or myelopathies at CTV margins or field gradients. This suggests our target volumes and blended gradients are appropriate for highly conformal three-dimensional planning.

ARTICLE HISTORY
Received 22 June 2017
Accepted 25 October 2017

Introduction

Craniospinal irradiation (CSI) is a quintessential component of curative treatment for several pediatric and adult central nervous system malignancies. Many patients requiring CSI are now treated with proton therapy due to the superior dosimetry compared to photon therapy [1–3]. However, proton therapy is not available for all CSI patients and as such, contemporary photon CSI techniques are still utilized. Conventional photon CSI treatment in the prone position with manual field junction shifts is cumbrous and highly susceptible to error due to geometrical uncertainties. Helical tomotherapy, volumetric modulated arc therapy and intensity modulated radiation therapy (IMRT) have been utilized to overcome the limitations associated with traditional photon CSI treatment [4–13].

Published contemporary photon CSI techniques demonstrate superior dose homogeneity across target volumes and improved sparing of organs at risk. However, many of these reports consist of retrospective plan generations in a small cohort of patients and emphasize the dosimetric advantages of these techniques compared to conventional techniques [4,5,7,8,10–12]. To the best of our knowledge, clinical efficacy and safety data for only one contemporary technique has been published [13,14]. This report describes outcomes in 34 CSI patients treated with a hybrid forward and inverse planned, supine IMRT technique.

Material and methods

Patients and statistics

An Institutional Review Board approved retrospective review of all patients who received supine, hybrid IMRT CSI at Mayo Clinic from 2009 to 2014 was performed. Pertinent patient, tumor, radiation therapy, treatment-associated toxicities and relapse information was extracted from patient records. Data were analyzed using JMP Statistical Software (Version 10, SAS Institute Inc., Cary, NC, USA). Overall survival (OS) was calculated from the start of radiation therapy to date of death or date of last patient contact. Event free survival (EFS) was calculated from the start of radiation therapy to first event

CONTACT Nadia N. Issa Laack laack.nadia@mayo.edu Department of Radiation Oncology, Mayo Clinic, 200 1st Street SW, Rochester, MN 55905, USA
Supplemental data for this article can be accessed here.

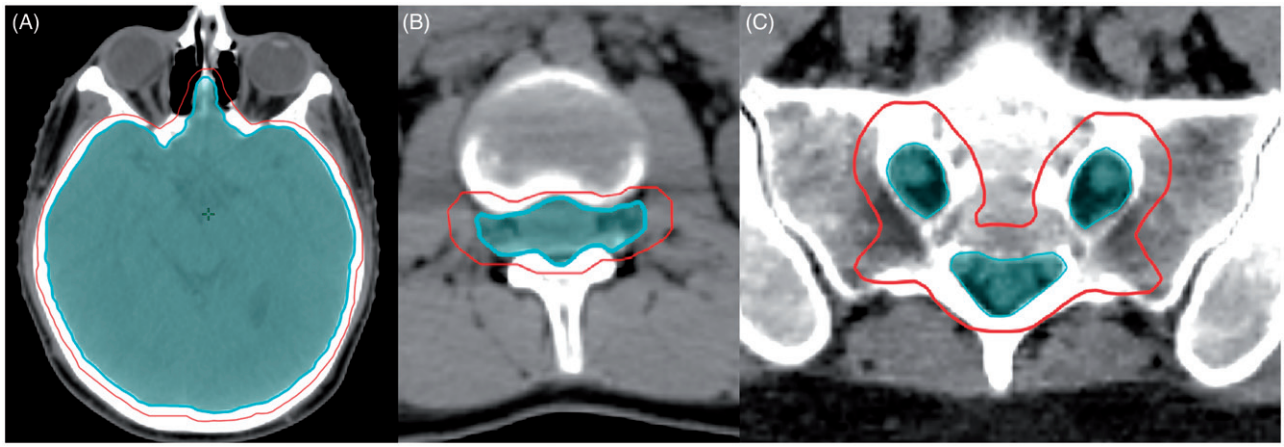

Figure 1. (A) Brain CTV and PTV at level of cribiform plate. CTV excludes intraconal optic nerves and globes. (B) Thecal sac CTV and PTV at level of lumbar spine. CTV includes nerve roots out to lateral edge of the vertebral body. (C) Thecal sac CTV and PTV at level of sacrum. Inner contours represent CTV. Outer contours represent PTV.

(recurrence or death) or date of last patient contact (censored). OS and EFS were calculated using the Kaplan–Meier method.

CSI technique

Patients were positioned supine during simulation with the head tipped back to move the oral cavity away from the upper spine. A head and shoulder thermoplastic mask with a headrest was used for immobilization. For patients requiring anesthesia, nasal cannula was inserted through the mask. For non-anesthesia patients, a bite block was used with the mask. Arms were placed at patients' sides. Patients were scanned with computed tomography (CT) and images were transferred to Eclipse treatment planning system (Varian Medical Systems, Palo Alto, CA).

Craniospinal clinical target volume (CTV) was defined as intracranial contents and thecal sac. Intracranial contents were contoured on bone windows with special attention to the cribiform plate and without inclusion of intraconal optic nerves or globes (Figure 1(A)). The thecal sac was defined as the spinal canal, including nerve roots terminating at the lateral border of the vertebral bodies and sacral nerve roots (Figure 1(B,C)). The planning target volume (PTV) was a two mm expansion on intracranial CTV at the cribiform plate and orbit, and a 5 mm expansion for remaining intracranial CTV. The PTV expansion for thecal sac CTV was 3–5 mm anteriorly and posteriorly, and 5–8 mm right, left and inferiorly depending on patient age and size. Dose was prescribed such that >95% of PTV received >95% of prescription dose and >99% of CTV received >99% of prescription, with no attempt to include vertebral bodies.

The Varian linear accelerator is equipped with multileaf collimator (MLC) leaves with 5 mm width at the center and 10 mm peripherally. Six megavoltage photons were used for all fields. Lateral fields were utilized for the cranium and upper cervical spine (Figure 2(A)). Isocenter was set so that the inferior cranium field borders fell just above the patients' shoulders. The gantry could be rotated slightly to eliminate divergence at the lens. The inferior Y jaw of the fields was set at 10 cm. A straight posterior beam with a source to surface distance of 130 cm was used for the upper spine field (Figure 2(B–D)). The superior Y jaw was set to 10 cm. The beam was aligned such that the superior jaw was just below the oral cavity. If less than 6 cm of overlap existed between the cranium and upper spine fields, the couch was turned to 90° and gantry tilted to a slightly superior angle, or the beam was moved superiorly so a small portion of the beam exited through the oral cavity. The inferior Y jaw was set to 10 cm, but could be extended to cover the entire spine. A straight posterior inferior spine field was used, if needed, with the same source to surface distance, couch height, and lateral position as the upper spine field. The beam overlapped approximately 10–15 cm with the upper spine field. The inferior jaw completely covered the lower spine. If the straight posterior spine field(s) resulted in significant hot spots posteriorly, two to three oblique fields were used (Supplementary Figure 1). Oblique spine fields also allowed for improved cardiac sparing compared to straight posterior spine field(s). Oblique spine fields were more commonly utilized in adult patients treated to 36.0 Gy.

Plans were generated with a hybrid of forward and inverse planned multiple static segment IMRT delivery. Specifically, the cranium fields were forward planned. The dose through physician-defined MLC apertures was calculated and field-in-field (FIF) apertures were added to compensate for dose heterogeneities. Long, smooth dose gradients in the cranium and upper spine fields overlap region was created with new FIF segments from each of the largest cranium aperture fields while closing the most inferior MLC leaf pairs in the new segment. A fraction of weight was then redirected from the full apertures to the new segment. Another set of FIF segments was created while closing the next inferior leaf pair. This process was repeated until a 6 cm long, smooth dose gradient covered the region from the shoulders to the oral cavity. All segments were equally weighted through the gradient.

For the lower spine field(s), a temporary gradient involving the inferior portion of the superior spine field(s) was first created in a fashion similar to the gradient involving the cranium fields. A FIF segment from the full aperture beam was created while closing the most superior leaf pair, and a

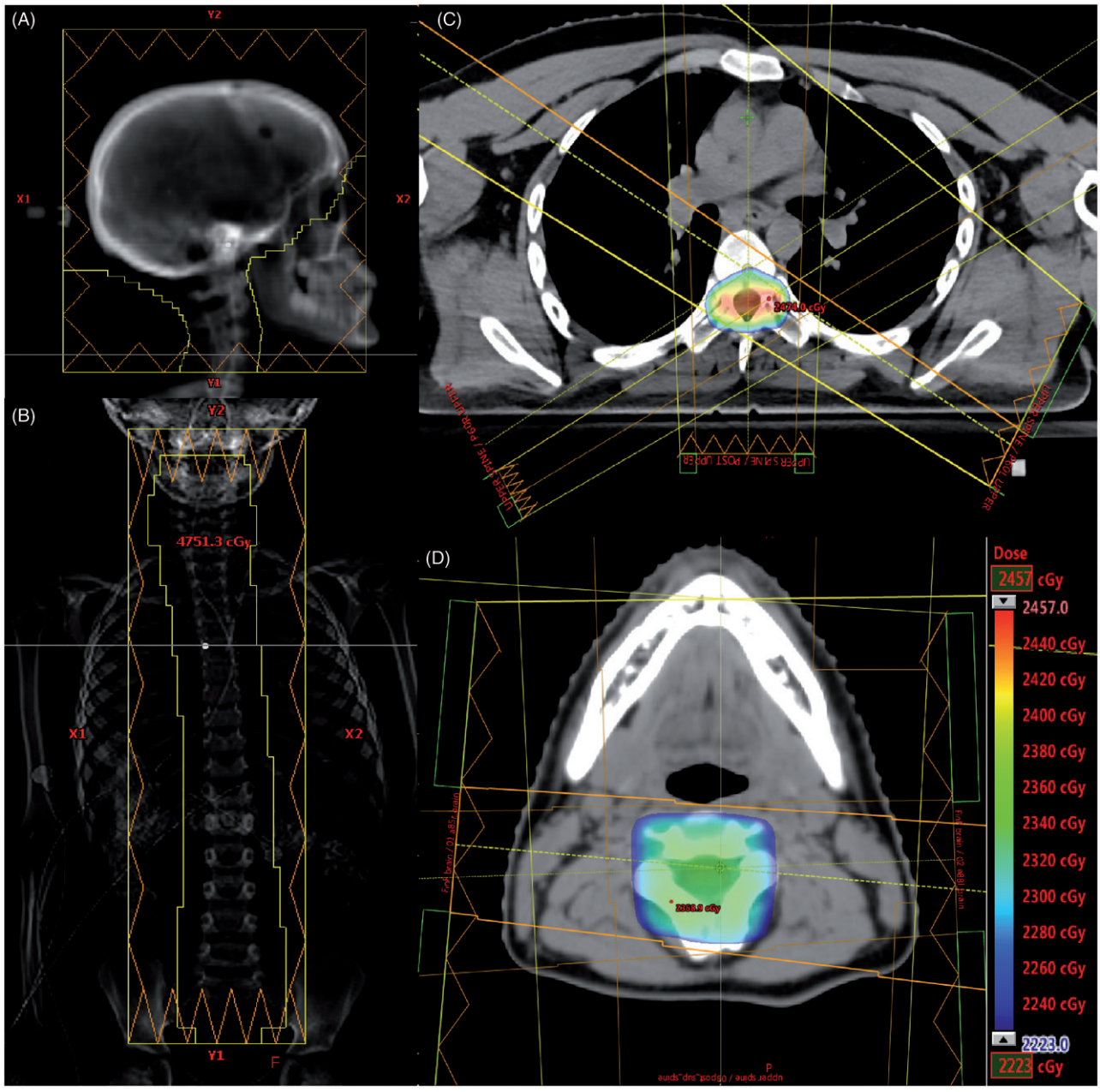

Figure 2. (A) Right lateral cranial field. (B) Single straight posterior spine field. (C) Axial image of dose from three spine fields (one straight posterior and two obliques). (D) Axial image of dose at cranial fields and posterior upper spine field overlap region. The dose color wash legend displays dose from 95% to 105% of 23.4 Gy. The legend is applicable to C and D.

fraction of weight was redirected from the full aperture to the new segment. These steps were repeated with more leaf pairs until a 10–15 cm dose gradient was created. The forward planned cranium fields and the temporary lower spine field(s) gradient were summed and used as the base plan for inverse planning of the superior spine field. The sliding window upper spine IMRT field was created by the inverse planning system to match gradients of the cranium and lower spine fields. FIF segment weights were adjusted and/or new segments added to smooth the dose distribution if needed. The lower spine field gradient was completed in a similar fashion using the forward planned cranium fields summed with the inversely planned upper spine field as a base plan. The final CSI plan summed the cranium, upper spine and lower spine fields (Figure 3). The objective for organs at risk was to minimize dose as much as possible without compromising target coverage.

A spreadsheet was created with isocenter coordinates for all fields in a patient's plan. Onboard kilovoltage imaging confirmed patient alignment and location prior to treatment each day. The spreadsheet provided couch coordinates for both upper and lower spine fields after the cranial coordinates were determined from imaging. Patient specific quality assurance was performed before the first treatment fraction by measuring cumulative plan doses with a MatriXX ion chamber array (IBA Dosimetry, Louvain-la-Neuve, Belgium). Measurements were performed for each plan with the MatriXX array positioned in the cranial/upper spine junction and again in the upper spine/lower spine junction, if applicable. Cerrobend blocks were placed under the MatriXX

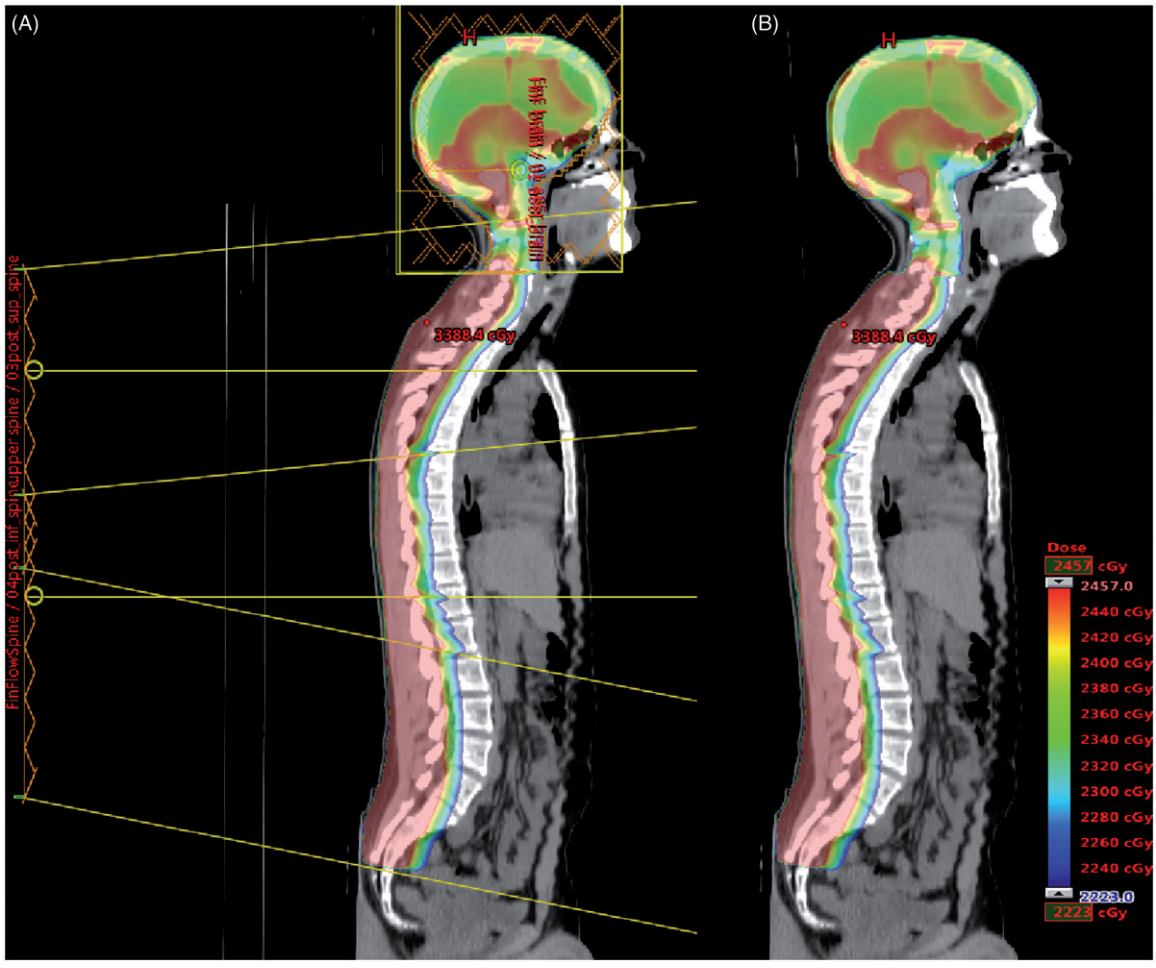

Figure 3. CSI plan for 23.4 Gy prescription dose with field orientation (A) and without field orientation (B). The dose color wash legend displays dose from 95% to 105% of 23.4 Gy. The legend is applicable to A and B.

electronics to shield them from posterior spine fields during measurement, and the patient's isocenter coordinate spreadsheet was used to shift the MatriXX during quality assurance to verify proper field design and couch coordinate shifts. Both cumulative plan doses and individual field gradients were compared to the planning system calculation with a 3% dose criterion for all pixels in the treatment fields. In addition to ion chamber array measurements, a secondary dose calculation was performed for each field using RadCalc software (LSI Software, Austin, TX) with a passing criterion of 2% (Supplementary Figure 2).

Results

Thirty-four patients were included in the analysis. Histologies included 19 medulloblastomas, eight primitive neuroectodermal tumors, four germ cell tumors, one pineoblastoma, one anaplastic ganglioglioma and one atypical teratoid/rhabdoid tumor. Median age at diagnosis was 15.3 years (range: 2.3–65.4 years). CSI prescription dose was 23.4 Gy in 11 patients, 36.0 Gy in 20 patients, 18.0 Gy in one patient, 34.2 Gy in one patient and 39.6 Gy in one patient. The median boost dose was 55.8 Gy (range: 30.6–60 Gy).

Median *V* 99% was 99.8% (range: 97.45–100.0%) for CTV 23.4 Gy and 99.7% (range: 92.7–100%) for CTV 36.0 Gy. Median *V* 95% was 97.9% (range: 90.8–100%) for PTV 23.4 Gy and 99.4% (range: 86.5–100%) for PTV 36.0 Gy. CTV *V* 99% was >99% and PTV *V* 95% was >95% for the three patients treated to non-23.4 Gy/36.0 Gy doses. Median *V* 105% was 18.3% (range: 5.2–33.7%) for PTV 23.4 Gy and 20.6% (range: 3.7–37.0%) for PTV 36.0 Gy. To verify the robustness and safety of the CSI plans, dose was calculated assuming a systematic set-up error of 3 mm. Resulting dose errors were ±15%.

Dose–volume data for organs at risk with 23.4 Gy and 36.0 Gy CSI doses are listed in Supplementary Tables 1 and 2. For growing patients (<16 years of age), the median mean vertebral body dose was 22.8 Gy (range: 21.7–23.31 Gy) with 23.4 Gy prescription dose and 34.4 Gy (range: 16.12–34.78 Gy) with 36.0 Gy prescription dose. The median mean value for vertebral body *V* 20 Gy was 99.7% for 23.4 Gy prescription dose and 100% for 36.0 Gy prescription dose.

With a median follow-up of 59.4 months (range: 3.2–89.2 months) in surviving patients, the five year OS was 86.0% (95% confidence interval (CI), 74.1–99.8%) and EFS was 66.7% (95% CI, 51.5–86.3%) for the entire cohort. Five year OS by histology was 100% for medulloblastoma, 50.0% for PNET and 100% for remaining tumors. Five year EFS was 80.2% for medulloblastoma, 25.0% for PNET and 85.7% for remaining histologies. Eleven patients had recurrence, all of which were

intracranial (Table 1). Four recurrences occurred out-of-field in relation to boost volumes. One average risk medulloblastoma patient presented 5.8 years after treatment with hemorrhage within the posterior fossa at the peripheral margin of the intracranial boost volume. Subsequent imaging suggested possible underlying mass, which was located in the 39.0 Gy isodose line for the boost volume. The median time to recurrence was 1.6 years (range: 0.6–5.8 years). There were no isolated recurrences at CTV margins or field gradients.

Table 2 lists treatment-associated toxicities as mentioned in patient charts. No spinal myelopathies were seen. The patient with scoliosis was diagnosed with PNET at 7.9 years of age. CSI dose was 39.6 Gy and spine boost dose from T7-S2 was 45.0 Gy. Vertebral body *V* 30 Gy was 100%. The scoliosis was mentioned 1.2 years after start of radiation, and was managed with physical therapy.

Discussion

CSI is a challenging treatment requiring technical expertise in treatment planning and delivery to a large and complexly shaped target. Many changes in CSI treatment have transpired over the past decade aimed at improving target dose homogeneity, minimizing dose-dependent positional variations, improving patient comfort and reducing dose to organs at risk. Our hybrid forward and inverse planned, supine IMRT CSI technique contributes to the growing literature of contemporary photon CSI techniques. The technique can be utilized to treat children and adults, and is associated with suitable target volume coverage, reasonable dose errors with set-up deviations, and acceptable doses to organs at risk. More importantly, the results demonstrate this technique did not result in recurrences or myelopathies at CTV margins and field gradients, suggesting our target volumes and blended gradients are appropriate for highly conformal three-dimensional planning.

Contemporary CSI techniques eliminate several of the limitations associated with conventional treatment. Traditional techniques require patients be in the prone position in order to utilize skin surface markers to match adjacent fields and to manually shift field junctions during treatment. This interfractional 'feathering' of field junctions creates sensitive dose gradients that produce inadvertent hot or cold spots in the spinal canal with positional variations [15]. Our technique tackles the traditional field junction pitfalls by overlapping adjacent fields and using MLC and FIF apertures to blend dose across the junctions. This approach results in at least a 6 cm dose gradient that is less susceptible to longitudinal positional variations. Our technique also improves upon treatment efficiency by only utilizing longitudinal couch shifts for imaging and treatment, compared to couch shifts and rotations required with traditional techniques. Finally, the supine position is more comfortable for patients and allows for easier airway access for pediatric patients requiring anesthesia.

Some published IMRT CSI techniques utilized helical tomotherapy and volumetric arc therapy to overcome the challenges associated with conventional treatment [4,6,12,16,17]. Arc therapy certainly addresses field junction issues, but can deliver a high integral dose to normal tissues [16]. We purposely selected conventional treatment fields to minimize the low radiation doses delivered to normal tissues. The techniques published by Cao et al. and Kusters et al. share similarities with our method in that adjoining fields are overlapped and the resulting dose inhomogeneity is compensated through IMRT optimization [5,8]. However, multiple beam directions are required with these techniques. For instance, Kusters et al. utilized five coplanar beams for adjacent spine fields and Cao et al. used seven fields for the craniospinal junction [5,8]. The theoretical disadvantage of using several beam angles, again, is increased exposure of healthy tissues to low radiation doses. Our technique sometimes necessitated multiple oblique spine fields if the straight posterior spine field(s) resulted in unacceptable posterior hot spots. However, the total number of spine fields never exceeded three and the beam arrangement was associated with improved cardiac sparing (Supplementary Figure 1). Yom et al. described a contemporary CSI technique using FIF homogenization and intrafractional modulation of field junctions, but patients remained in the prone position [15]. The techniques published by Seppala et al. and South et al. are similar to our technique in terms of field design and MLC-based field junction feathering [11,13]. The report by Seppala et al. is limited though in that the technique was applied retrospectively to five adult patients.

It is well known under-dosage of CSI target volumes correlates with increased risk of relapse [18–20]. Traditional techniques are highly susceptible to inadequate target coverage due to the geometrical uncertainties associated with adjoining fields, especially if setup misalignments occur. IMRT negates this uncertainty be creating gradients across field junctions that are less susceptible to setup uncertainties. Some published IMRT techniques, however, still utilize geometrically matched field junctions requiring interfractional feathering [9,10]. Therefore, clinical efficacy and safety data from contemporary CSI techniques are necessary. To the best of our knowledge, only one technique has reported clinical outcomes. South et al. did not report any failures at the brain-field or spine–spine field junctions in 23 patients with a median follow-up of 20.2 months [13]. The updated report with long-term follow-up documented a simultaneous recurrence in the brain and spinal cord close to a junction site in one patient [14]. In our cohort, all recurrences were intracranial, primarily in-field with regards to boost volumes. There were no recurrences at CSI CTV margins or field gradients. Our results and the reports of South et al.'s technique suggest appropriately designed IMRT dose gradients are associated with low risk of relapse at CSI field junctions. Conversely, patients may experience spinal myelopathy if misalignments result in an over-dosage within the treatment volume. As risk of spinal myelopathy correlates with dose per fraction [21], treatment involving smooth dose gradients across overlapping fields is less likely to result in the complication compared to treatment with sharp field junctions. There were no cases of spinal myelopathy in our cohort nor with the technique described by South et al. [13,14].

Table 1. Recurrence site(s) following craniospinal irradiation (CSI) and correlation to radiation plans.

Patient	Histology	Age at start of radiation (years)	CSI dose (Gy)	Intracranial boost dose (Gy)	Metastases and boost dose (Gy)	Recurrence site(s)	Time to recurrence (years)	Plan details relative to recurrence site(s)
1	Medulloblastoma	10.7	23.4	54.0	–	Left lateral ventricle	3.2	Recurrence within 23.4 Gy prescription isodose line
2	Medulloblastoma	17.2	23.4	54.0	–	Right lateral ventricle and septum pellucidum	1.5	Recurrences within 23.4 Gy prescription isodose line
3	Medulloblastoma	7.0	23.4	55.8	–	Hemorrhage with possible underlying mass within left cerebellar hemisphere	5.7	Mass within 39.0 Gy intracranial boost isodose line
4	PNET	64.4	36.0	55.8	–	Left frontoparietal area, along resection margin	1.0	Recurrence within 55.8 Gy prescription isodose line
5	PNET	18.6	36.0	55.8	–	Left lateral ventricle, left parietal lobe, left cerebellar hemisphere, vermis	1.0	Left lateral ventricle recurrence within 55.8 Gy prescription isodose line. Remainder of recurrences within 36.0 Gy prescription isodose line
6	PNET	23.5	36.0	55.8	–	Right parietal lobe	1.6	Recurrence within 53.0–55.8 Gy intracranial boost isodose lines
7	PNET	21.4	36.0	55.8	–	Right frontal, parietal and temporal lobes; right lateral ventricle	0.5	All recurrences within 55.8 Gy prescription isodose line
8	PNET	65.5	36.0	60.0	–	Right lateral ventricle, thalamus and external capsule	1.4	All recurrences within 57.0–60.0 Gy intracranial boost isodose lines
9	PNET	8.0	39.6	55.8	Diffuse leptomeningeal enhancement, most prominent at T7-8; 45.0 Gy T7-S2	Right cerebellar hemisphere	3.1	Recurrence within 39.6 Gy prescription isodose line
10	Medulloblastoma	34.0	36.0	55.8	N/A	Left cerebellar hemisphere	1.4	Recurrence within 55.8 Gy prescription isodose line
11	Pinealoblastoma	31.0	36.0	50.0 (Gamma knife)	N/A	Bilateral thalamic, midbrain, vermis, right cerebellar hemisphere	1.9	Recurrence within 17.5 Gy intracranial boost isodose line

Gy : Gray.

Table 2. Treatment-associated toxicities as mentioned in medical charts.

Patient	Histology	Age at start of radiation (years)	CSI dose (Gy)	Boost dose (Gy)	Toxicities	Time to toxicities from start of radiation (years)
1	Germinoma	14.6	23.4	30.6	Testing accommodations in college (Grade 1)	4.4
2	Medulloblastoma	13.7	36.0	54.0	(1) Azospermia (Grade 3)	(1) 0.7
					(2) Persistent left cerebellar dysfunction since start of radiation	(2) 0.0
3	Medulloblastoma	8.9	23.4	54.0	Hypothyroidism (Grade 2)	2.1
4	Medulloblastoma	10.7	23.4	54.0	(1) Memory and focus issues- 'easy distractability' (Grade 1)	(1) 5.3
					(2) Panhypopituitarism (Grade 2)	(2) 5.3
					(3) Osteopenia (Grade 1)	(3) 3.7
5	Medulloblastoma	7.6	23.4	54.0	Left-sided dysmetria, balance issues (Grade 1)	1.2
6	Medulloblastoma	24.8	23.4	55.8	(1) Peripheral neuropathy (Grade 1)	(1) 0.9
					(2) Erectile dysfunction (Grade 1)	(2) 2.9
					(3) Azoospermia (Grade 3)	(3) 2.9
7	Medulloblastoma	27.3	36.0	55.8	Amenorrhea (Grade 1)	1.1
8	Medulloblastoma	33.1	34.2	54.0	Gait instability, left-sided incoordination (Grade 2)	0.8
9	Medulloblastoma	36.1	36.0	55.8	(1) Gait unsteadiness (Grade 1)	(1) 0.7
					(2) Right extremity ataxia (Grade 1)	(2) 0.7
10	Medulloblastoma	6.1	23.4	55.8	(1) Bilateral cataracts (Grade 1)	(1) 3.5
					(2) Hearing loss (Grade 3)	(2) 1.5
					(3) Growth hormone deficiency (Grade 2)	(3) 2.0
					(4) Requires special education (Grade 2)	(4) 3.0
11	Medulloblastoma	7.0	23.4	55.8	(1) Bilateral cataracts (Grade 3)	(1) 1.4
					(2) Growth hormone deficiency (Grade 3) Myelodysplastic syndrome	(2) 3.4 (3) 4.5
12	Medulloblastoma	29.7	36.0	54.0	Short-term memory difficulties (Grade 1)	0.7
13	Medulloblastoma	6.3	23.4	55.8	(1) Bilateral cataracts (Grade 3)	1) 2.7
					(2) Hypothyroidism (Grade 2)	2) 4.7
14	ATRT	4.2	36.0	54.0	(1) Hearing loss (Grade 3)	(1) 1.2
					(2) Persistent ataxia since start of radiation (Grade 1)	(2) 0.0
					(3) Hypothyroidism (Grade 2)	(3) 1.6
15	PNET	7.9	36.0	55.8	(1) Hypothyroidism (Grade 2)	(1) 0.7
					(2) Hearing loss (Grade 1)	(2) 1.2
					(3) Poor growth velocity (Grade 1)	(3) 2.2
16	PNET	18.6	36.0	55.8	(1) Hearing loss (Grade 1)	(1) 3.3
					(2) Bilateral cataracts (Grade 3)	(2) 3.8
					(3) Ovarian failure (Grade 3)	(3) 3.6
17	PNET	65.6	36.0	60.0	Poor short-term memory (Grade 1)	1.5
18	PNET	6.8	36.0	55.8	(1) Bilateral cataracts (Grade 3)	(1) 2.9
					(2) Hypothyroidism (Grade 2)	(2) 1.5
					(3) Hypoadrenalism (Grade 2)	(3) 1.5
					(4) Decreased growth (Grade 3)	(4) 2.9
					(5) 2 years behind in school (Grade 3)	(5) 2.9
19	PNET	80	39.6	55.8	(1) Hypothyroidism (Grade 2)	(1) 1.2
					(1) Scoliosis (40°) (Grade 2)	(2) 1.2
20	Medulloblastoma	34.0	36.0	55.8	(1) Gait instability present since start of radiation (Grade 1)	(1) 0.0
					(2) Dysarthria and dysphagia when fatigued (Grade 1)	(2) 4.2
					(3) Bilateral cataracts (Grade 3)	(3) 4.2
21	Germinoma	12.8	23.4	32.4	Panhypopituitarism (Grade 3)	0.5
22	Anaplastic ganglioglioma	11.0	36.0	50.4	Ovarian failure (Grade 3)	1.7
23	Germinoma	15.2	36.0	54.0	Bilateral hearing loss (Grade 1)	0.1

Toxicities are graded per Common Terminology Criteria for Adverse Events, version 4.0. Gy : Gray.

In the two-dimensional planning era, CSI treatment fields were designed based on bony landmarks. There is no consensus regarding optimal target volumes with CT-based planning. The outcomes associated with our technique suggest our target volumes are appropriate for highly conformal three-dimensional planning. Our treatment volumes excluded intraconal optic nerves. The entire length of the optic nerves is typically targeted by cranial fields because the nerves are enveloped by cerebrospinal fluid and are in the beam path directed at the cribiform plate. The advantage of excluding the intraconal optic nerves is added leverage to minimize dose to the globes. The lateral extent of our thecal sac CTV is smaller than historically treated volumes, especially near the sacrum where minimal widening is appreciated (Figure 2(B)). Vertebral bodies are usually targeted in growing patients to avoid dose gradients that may result in vertebral body deformation. Efforts to reduce vertebral body dose may be beneficial for patients, though, as data suggests mean vertebral dose is associated with hematologic toxicity [22]. We intentionally excluded vertebral bodies from our treatment volume to minimize dose as much as possible. However, we optimized plans for a homogenous dose gradient across vertebral bodies, especially in growing patients, to minimize subsequent vertebral body wedging and scoliosis due to dose asymmetry. Only one patient experienced scoliosis in our cohort. The *V* 30 Gy was 100% across vertebral bodies; however, the patient received a high dose boost from T7-S2 for diffuse leptomeningeal enhancement.

In conclusion, the data presented here demonstrate the safety and efficacy of our hybrid forward and inverse planned, supine IMRT CSI technique. Though this study is limited in its retrospective nature, it adds to the current literature as an outcomes report for a contemporary CSI technique. The results suggest our target volumes and blended gradients are suitable for highly conformal three-dimensional planning.

Disclosure statement

The authors report no conflicts of interest.

ORCID

Nadia N. Issa Laack http://orcid.org/0000-0002-4385-6349

References

[1] St Clair WH, Adams JA, Bues M, et al. Advantage of protons compared to conventional X-ray or IMRT in the treatment of a pediatric patient with medulloblastoma. Int J Radiat Oncol Biol Phys. 2004;58:727–734.

[2] Mu X, Bjork-Eriksson T, Nill S, et al. Does electron and proton therapy reduce the risk of radiation induced cancer after spinal irradiation for childhood medulloblastoma? A comparative treatment planning study. Acta Oncol. 2005;44:554–562.

[3] Brodin NP, Munck A, Rosenschold P, et al. Radiobiological risk estimates of adverse events and secondary cancer for proton and photon radiation therapy of pediatric medulloblastoma. Acta Oncol. 2011;50:806–816.

[4] Bedford JL, Lee YK, Saran FH, et al. Helical volumetric modulated arc therapy for treatment of craniospinal axis. Int J Radiat Oncol Biol Phys. 2012;83:1047–1054.

[5] Cao F, Ramaseshan R, Corns R, et al. A three-isocenter jagged-junction IMRT approach for craniospinal irradiation without beam edge matching for field junctions. Int J Radiat Oncol Biol Phys. 2012;84:648–654.

[6] Fogliata A, Bergstrom S, Cafaro I, et al. Cranio-spinal irradiation with volumetric modulated arc therapy: a multi-institutional treatment experience. Radiother Oncol. 2011;99:79–85.

[7] Howell RM, Giebeler A, Koontz-Raisig W, et al. Comparison of therapeutic dosimetric data from passively scattered proton and photon craniospinal irradiations for medulloblastoma. Radiat Oncol. 2012;7:116.

[8] Kusters JM, Louwe RJ, van Kollenburg PG, et al. Optimal normal tissue sparing in craniospinal axis irradiation using IMRT with daily intrafractionally modulated junction(s). Int J Radiat Oncol Biol Phys. 2011;81:1405–1414.

[9] Pai Panandiker A, Ning H, Likhacheva A, et al. Craniospinal irradiation with spinal IMRT to improve target homogeneity. Int J Radiat Oncol Biol Phys. 2007;68:1402–1409.

[10] Parker W, Filion E, Roberge D, et al. Intensity-modulated radiotherapy for craniospinal irradiation: target volume considerations, dose constraints, and competing risks. Int J Radiat Oncol Biol Phys. 2007;69:251–257.

[11] Seppala J, Kulmala J, Lindholm P, et al. A method to improve target dose homogeneity of craniospinal irradiation using dynamic split field IMRT. Radiother Oncol. 2010;96:209–215.

[12] Sharma DS, Gupta T, Jalali R, et al. High-precision radiotherapy for craniospinal irradiation: evaluation of three-dimensional conformal radiotherapy, intensity-modulated radiation therapy and helical TomoTherapy. BJR. 2009;82:1000–1009.

[13] South M, Chiu JK, Teh BS, et al. Supine craniospinal irradiation using intrafractional junction shifts and field-in-field dose shaping: early experience at Methodist Hospital. Int J Radiat Oncol Biol Phys. 2008;71:477–483.

[14] Verma J, Mazloom A, Teh BS, et al. Comparison of supine and prone craniospinal irradiation in children with medulloblastoma. Pract Radiat Oncol. 2015;5:93–98.

[15] Yom SS, Frija EK, Mahajan A, et al. Field-in-field technique with intrafractionally modulated junction shifts for craniospinal irradiation. Int J Radiat Oncol Biol Phys. 2007;69:1193–1198.

[16] Bandurska-Luque A, Piotrowski T, Skrobala A, et al. Prospective study on dosimetric comparison of helical tomotherapy and 3DCRT for craniospinal irradiation – a single institution experience. Rep Pract Oncol Radiother. 2015;20:145–152.

[17] Myers P, Stathakis S, Mavroidis P, et al. Evaluation of localization errors for craniospinal axis irradiation delivery using volume modulated arc therapy and proposal of a technique to minimize such errors. Radiother Oncol. 2013;108:107–113.

[18] Carrie C, Hoffstetter S, Gomez F, et al. Impact of targeting deviations on outcome in medulloblastoma: study of the French Society of Pediatric Oncology (SFOP). Int J Radiat Oncol Biol Phys. 1999;45:435–439.

[19] Chojnacka M, Skowronska-Gardas A. Medulloblastoma in childhood: impact of radiation technique upon the outcome of treatment. Pediatr Blood Cancer. 2004;42:155–160.

[20] Miralbell R, Bleher A, Huguenin P, et al. Pediatric medulloblastoma: radiation treatment technique and patterns of failure. Int J Radiat Oncol Biol Phys. 1997;37:523–529.

[21] Kirkpatrick JP, van der Kogel AJ, Schultheiss TE. Radiation dose-volume effects in the spinal cord. Int J Radiat Oncol Biol Phys. 2010;76:S42–S49.

[22] Brown AP, Barney CL, Grosshans DR, et al. Proton beam craniospinal irradiation reduces acute toxicity for adults with medulloblastoma. Int J Radiat Oncol Biol Phys. 2013;86:277–284.